NASA/TM–2010-216696

A Two-Axis Direct Fluid Shear Stress Sensor

Edward E. Adcock and Michael A. Scott
Langley Research Center, Hampton, Virginia

Sateesh S. Bajikar
QSS Group, Inc., Greenbelt Maryland

May 2010

NASA STI Program . . . in Profile

Since its founding, NASA has been dedicated to the advancement of aeronautics and space science. The NASA scientific and technical information (STI) program plays a key part in helping NASA maintain this important role.

The NASA STI program operates under the auspices of the Agency Chief Information Officer. It collects, organizes, provides for archiving, and disseminates NASA's STI. The NASA STI program provides access to the NASA Aeronautics and Space Database and its public interface, the NASA Technical Report Server, thus providing one of the largest collections of aeronautical and space science STI in the world. Results are published in both non-NASA channels and by NASA in the NASA STI Report Series, which includes the following report types:

- TECHNICAL PUBLICATION. Reports of completed research or a major significant phase of research that present the results of NASA programs and include extensive data or theoretical analysis. Includes compilations of significant scientific and technical data and information deemed to be of continuing reference value. NASA counterpart of peer-reviewed formal professional papers, but having less stringent limitations on manuscript length and extent of graphic presentations.

- TECHNICAL MEMORANDUM. Scientific and technical findings that are preliminary or of specialized interest, e.g., quick release reports, working papers, and bibliographies that contain minimal annotation. Does not contain extensive analysis.

- CONTRACTOR REPORT. Scientific and technical findings by NASA-sponsored contractors and grantees.

- CONFERENCE PUBLICATION. Collected papers from scientific and technical conferences, symposia, seminars, or other meetings sponsored or co-sponsored by NASA.

- SPECIAL PUBLICATION. Scientific, technical, or historical information from NASA programs, projects, and missions, often concerned with subjects having substantial public interest.

- TECHNICAL TRANSLATION. English-language translations of foreign scientific and technical material pertinent to NASA's mission.

Specialized services also include creating custom thesauri, building customized databases, and organizing and publishing research results.

For more information about the NASA STI program, see the following:

- Access the NASA STI program home page at *http://www.sti.nasa.gov*

- E-mail your question via the Internet to help@sti.nasa.gov

- Fax your question to the NASA STI Help Desk at 443-757-5803

- Phone the NASA STI Help Desk at 443-757-5802

- Write to:
  NASA STI Help Desk
  NASA Center for AeroSpace Information
  7115 Standard Drive
  Hanover, MD 21076-1320

NASA/TM–2010-216696

A Two-Axis Direct Fluid Shear Stress Sensor

Edward E. Adcock and Michael A. Scott
Langley Research Center, Hampton, Virginia

Sateesh S. Bajikar
QSS Group, Inc., Greenbelt Maryland

National Aeronautics and
Space Administration

Langley Research Center
Hampton, Virginia 23681-2199

May 2010

Available from:

NASA Center for AeroSpace Information
7115 Standard Drive
Hanover, MD 21076-1320
443-757-5802

Contents

List of Figures

Abstract

This innovation is a miniature or micro sized semiconductor sensor design that provides two axis direct non-intrusive measurement of skin friction or wall shear stress in fluid flow. The sensor is fabricated by micro-electro-mechanical system (MEMS) technology, enabling small size and low cost reproductions. The sensors have been fabricated by utilizing MEMS fabrication processes to bond a sensing element wafer to a fluid coupling wafer. This layering technique provides for an out of plane dimension that is on the same order of length as the in-plane dimensions. The sensor design has the following characteristics: a shear force collecting plate with dimensions that can be tailored to various application specific requirements such as spatial resolution, temporal resolution and shear force range and resolution. This plate is located coplanar to both the sensor body and flow boundary, and is connected to a dual axis gimbal structure by a connecting column or lever arm. The dual axis gimbal structure has torsional hinges with embedded piezoresistive torsional strain gauges which provide a voltage output that is correlated to the applied shear stress (and excitation current) on force collection plate that is located on the flow boundary surface (hence the transduction method). This combination of design elements create a "force concentration and resolution" structure that enables the generation of a large stress on the strain gauge from the small shear stress on the flow boundary wall. This design as well as the use of back side electrical contacts establishes a non-intrusive method to quantitatively measure the shear force vector on aerodynamic bodies.

Introduction

The measurement of shear stress is of importance in a large number of situations involving fluid flow, including aerodynamics, hydrodynamics, turbo-machinery, and polymer processing among others [1-7]. Quantifying shear stress is important in order to understand and control the flow and in particular to control and suppress the development of turbulence in it [10]. Shear stress measurement is also needed to provide a transfer standard for Computational Fluid Dynamics (CFD) validation, especially for complex turbulent flows [12]. The magnitude of the shear stress and needed resolution in these various situations can span many orders from milliPascals to kiloPascals or more. The frequency response and spatial resolution needed also varies considerably. Sensors employing direct and indirect principles for sensing shear force exist, with the direct methods being favored, however no commercial devices are readily available [11]. The requirements associated with sensors for aerodynamic applications are very challenging due to the fact that forces involved are small (few Pascal to few hundred Pascal). In addition the resolution of shear force needed is high (few milliPascal), the spatial resolution required is on the order of a few hundred microns or less, and the frequency response varies from steady state to tens of kilohertz [6].

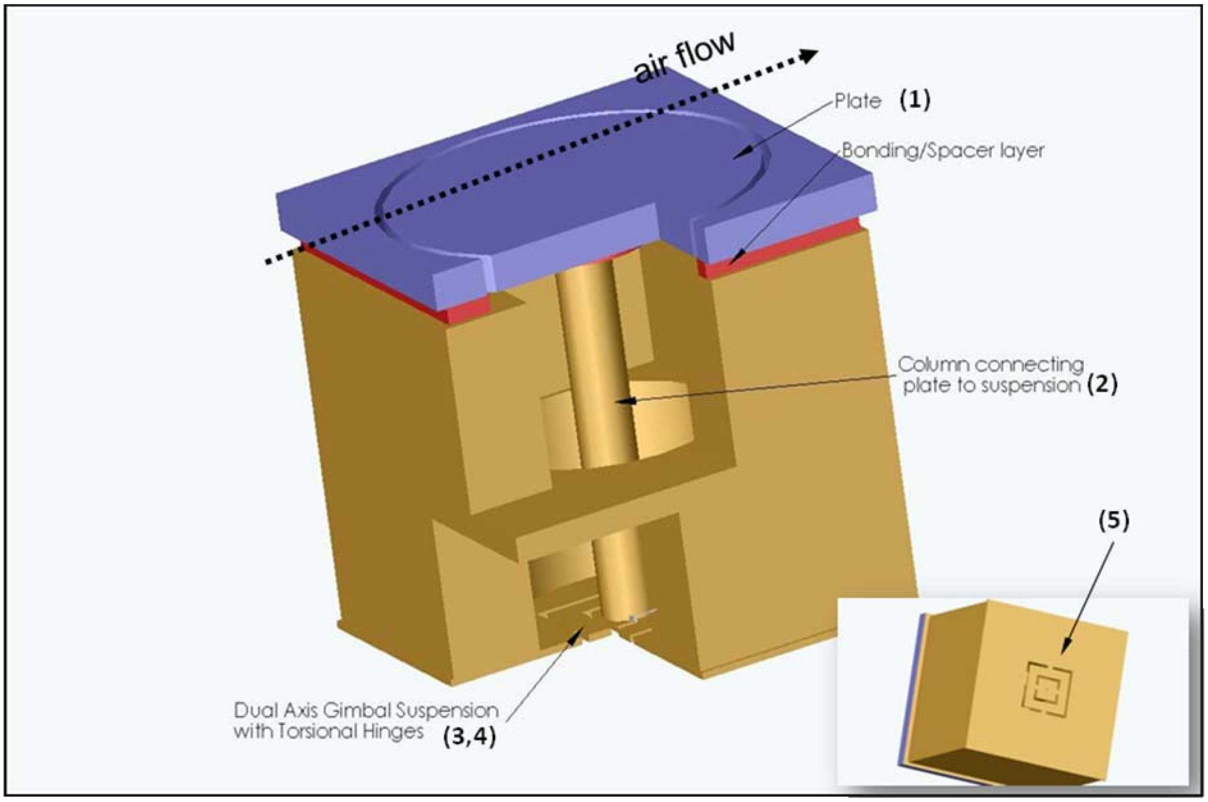

Figure 1. Cutaway View of Shear Stress Sensor

There is also the need for directional information that requires arrays of sensors to collect shear data over the area of interest. The present invention is a microsensor that is ideally suited for this application and has been fabricated using MEMS (Micro Electro Mechanical Systems) fabrication techniques. It is however not limited to this application and has many other uses that can be achieved by modifying the design parameters.

Description of Sensor

The shear sensor uses a plate that is flush with the sensor body and the flow boundary to "collect" the shear stress and couples it, using a lever arm, to a two axis torsional hinge gimbal structure. The gimbals have embedded piezoresistive sensors to provide an electrical signal that is proportional to the mechanical torsional shear stress they are experiencing (which in turn is proportional to the shear stress at the sensor plate). This configuration enables small fluid shear stresses to be measured by providing relatively large collection areas to accumulate a reasonable force and using an arm to transfer this to a large mechanical stress that can be easily measured with a piezoresistive sensor.

A cutaway view of the shear sensor is shown in Fig.1. The device is comprised of a plate (Fig.1, 1) that "collects" the shear force and is of a dimension comparable to the needed spatial resolution (10 to 100 to 1000s of microns depending on application). Its surface is coplanar and flush with the surface of the device body in order to enable non-intrusive or non disruptive mounting in the flow being probed. This plate is coupled to the arm (Fig. 1, 2) of a two axis gimbal structure (Fig.1, 3). These gimbals are torsional hinges (Fig.1, 4) and permit rotation of the arm (and plate) about both axes of the gimbal plane. This structure, consisting of the plate, arm, and gimbal, are designed such that the tilt of the plate does not impact the macroscopic flow parameters. The hinges are fabricated of single crystal silicon with embedded piezoresistive torsional sensors (Fig.1, 5). The sensor structure is shown in Fig. 2, and when excited with a suitable electrical current across terminals 1-2 the sensor outputs a voltage from contacts 3-4 proportional to the shear stress experienced by the hinge. The sensors themselves are typically made by doping the silicon (by ion implantation or other means) to a suitable type and level of conductivity that provides the desired sensitivity depending on the crystal orientation and confines the excitation current to the sensor. Metallic electrical leads (not shown) on the back face of the device are provided to route excitation currents and output signal voltages from these sensors to the external world. Subjecting the plate of the device (Fig.1, 1) to a shear force by mounting it on an aerodynamic surface exposed to flow will result in a moment acting on the hinges that is proportional to the shear stress on the plate and the plate arm and torsional hinge dimensions. This moment creates a mechanical torsional shear stress within the hinges and thereby an output signal proportional to the shear stress on the plate from the piezoresistive sensor. The shear stress at the fluid-sensor interface is initially converted to a mechanical shear stress in the hinge that is sensed with the piezoresistive sensor. The two orthogonally located hinges and sensors enable measuring the shear stress existing on the plate in both directions. This configuration of the sensor device enables a large moment and stress level to be generated at the hinge from relatively small shear stress acting on a small plate thereby enabling high spatial and stress resolution capability. The location of the piezoresistive sensor on the rear face of the device enables wiring in a non-intrusive manner which is important in applications where the aerodynamic flow is not to be disturbed. That is to say, all electrical contacts are below the flow surface. The entire device may be fabricated in single crystal silicon using two silicon or SOI (Silicon-On-Insulator) wafers which allows for fabrication of large arrays of sensors.

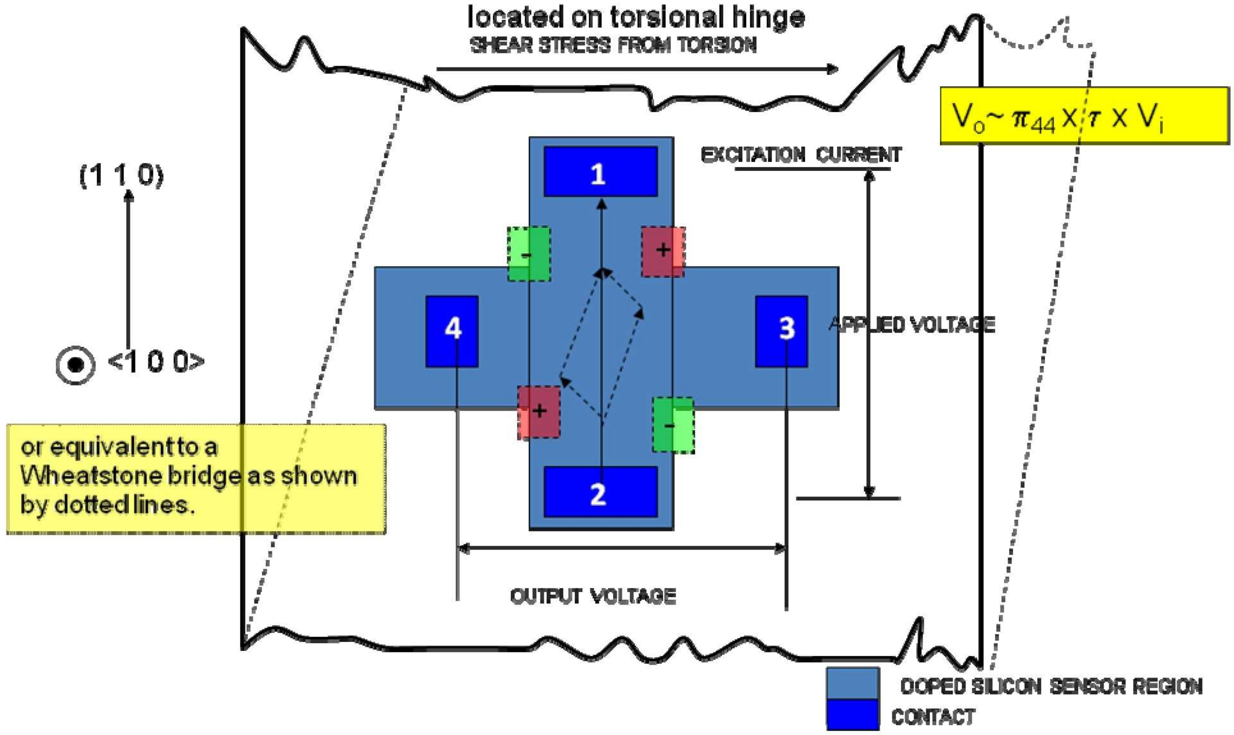

Figure 2. Shear/Torsion Piezoresistive Sensor

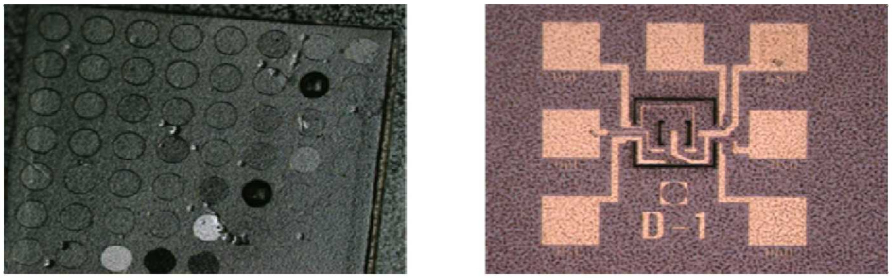

8x8 array, 430μm plate

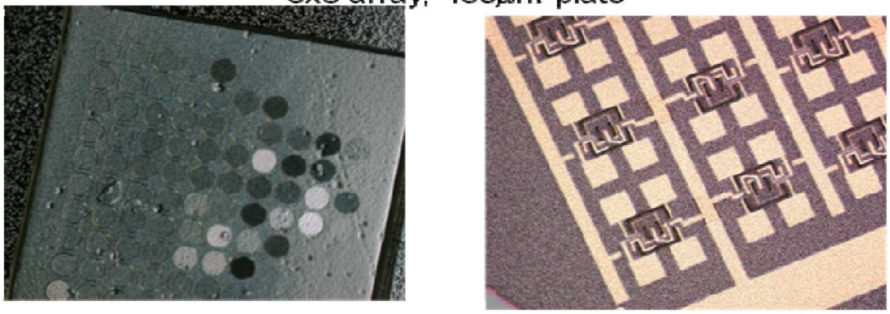

10x10 array, 320μm plate

Figure 3. Micrograph of Fabricated Sensors

The sensor is fabricated by bonding together two partially structured wafers. The first is processed to define the piezoresistive structures and metallic leads for the piezoresistive structures, using standard semiconductor ion implantation, deposition, lithography and etch techniques. The lever structure on the back side of this wafer is defined using photolithography and a deep silicon reactive ion etch using the BOSCH process [8] that stops on the buried oxide layer if present or is timed to desired depth. The second wafer is similarly processed to define plate or lever (lever optional depending on process and design), on its backside. The two wafers are aligned and bonded at a modest temperature and pressure compatible with the metals and other materials used. In addition an intermediary layer such as a polymer (e.g. BCB, polyimide, negative photoresist), metal (Gold-gold/ Si-gold eutectic) or glass is used during bonding. Additional lithography and silicon reactive ion etching steps define the plate and the hinge and gimbal on either side of the bonded wafers and completes the sensor. Figure 3 depicts a set of micrographs of the fabricated sensors. The two pictures on the left show the flow side of two different size arrays. The two photos on the right show the gimbal structure as well as the back side contacts.

$$\tau_{\omega} = \frac{h}{2}\frac{\delta p}{\delta l}$$

Equation 1

Experimantal Setup

Several of these sensors, of varying sensitivity and spatial resolution, have been fabricated and characterized. Table 1 shows the variety of sensors that were fabricated during the first fabrication process. The sensitivity depicted here is based on an approximate mechanical model; this model assumes that all deformation is concentrated at the hinges. The true sensitivity has proven to be up to two times lower when deformation of the frame is factored in. The maximum resolution model was based on the thermal noise limit; additional process-dependent noise sources will reduce the attainable resolution. Likewise, Table 2 shows the various sensors fabricated during the second fabrication process. One of the design criteria for the sensors included in Table 1 was high spatial resolution and these devices were fabricated with as many as 100 sensors on a 5 by 5cm silicon die. The sensors from the second fabrication run (Table 2) had a design criterion that focused on high yield and realistic back side contact wiring. Even so, these second generation sensors require 30 back-side electrical connections for a typical 4 sensor die. The number of sensors on each die was reduced to 4 and the die size was reduced to 3.5 by 3.5cm.

Design #	Plate Diameter (um)	Length of Lever (um)	Suspension Thickness (um)	Sensitivity mV/mA-Pa	Max. Resolution (Pa)	Range (Pa)	Fundamental Resonant Frequencies (~kHz)
1a	430	400	5	0.108	1/300	5700	40
1b	430	400	2	1.112	1/1700	390	10
2a	800	400	5	0.650	1/1000	1650	20
2b	800	400	2	3.800	1/5800	110	5
3a	1200	400	5	0.841	1/2250	740	11
3b	1200	400	2	8.650	1/12000	50	3
4a	140	400	5	0.002	1/30	54000	73
4b	140	400	2	0.118	1/180	3600	19
5a	340	400	5	0.118	1/180	9200	45
5b	340	400	2	0.695	1/1000	625	12

Table 1 First Fabricaion Design Summary

Design #	Plate Diameter (um)	Length of Lever (um)	Suspension Thickness (um)	Sensitivity mV/mA-Pa	Max. Resolution (Pa)	Range (Pa)	Fundamental Resonant Frequencies (~kHz)
1a	200	400	5	0.041	1/60	26000	65
1b	200	400	2	0.240	1/370	1800	17
2s	400	400	5	0.163	1/250	6600	42
2b	400	400	2	0.962	1/1450	450	11
3a	600	400	5	0.367	1/560	2900	28
3b	600	400	2	2.100	1/3300	200	7.5
4a	800	400	5	0.650	1/1000	1650	20
4b	800	400	2	3.800	1/5800	110	5

Table 2 Second Fabricaion Design Summary

The shear stress values were generated using a laminar flow channel (Fig. 4) and the sensors where mounted on the wall in an aerodynamically smooth manner as to not disturb the flow. The flow channel was designed to insure that

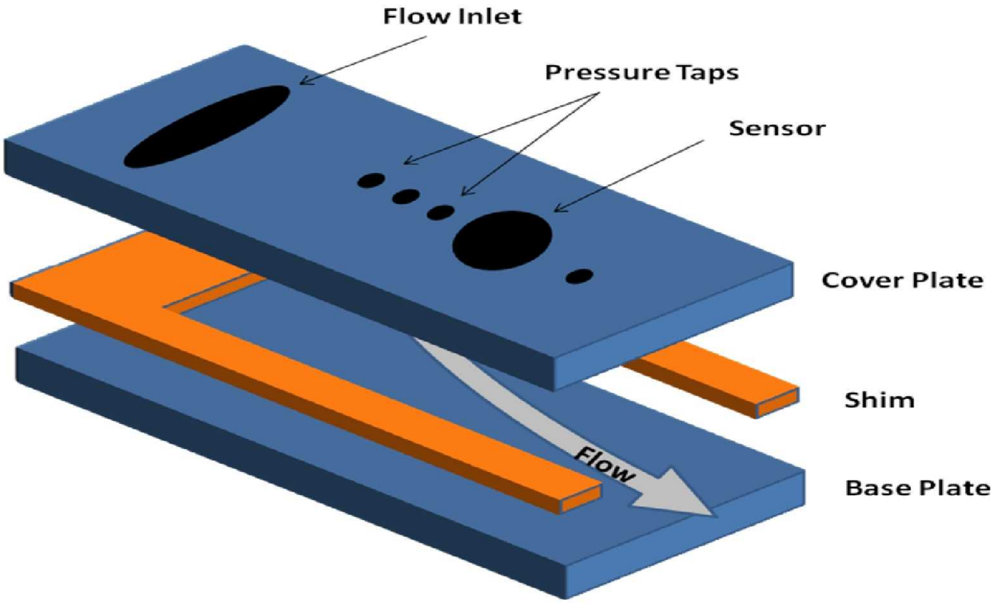

Figure 4. Laminar Flow Cell

$$Q = \frac{h^3 W}{12\mu} \frac{\delta p}{\delta l}$$

Equation 2

the flow will remain laminar during the entire tested shear range. This was done by using a pressure driven flow and a very high aspect ratio flow channel cross section (a few hundred microns by several centimeters) to insure a parabolic velocity distribution. This high aspect ratio also allows the use of a two dimensional flow model with negligible effects for the side walls. The shear stress was determined by measuring the pressure differential along the length of the channel, at several stations. Figure 4 depicts the pressure taps used to determine the pressure gradient; this figure also shows the location of the test article mounted in an indexed plug.

The shear stress at the wall in the laminar flow cell can be expressed using Equation 1, where τ_ω is the shear at the wall, h is the channel height, δp is the pressure drop along the channel, and δl is the pressure tap spacing [7]. The sensor mount as well as the pressure taps were cast into the channel using a low shrinkage epoxy to insure aerodynamic smoothness. Also the flow surfaces of the channel were laminated with a polished stainless steel surface to reduce flow perturbations. Volumetric flow rate was also measured as a secondary insurance that Equation 1 is valid for given flow conditions, by comparing results to Equation 2. Where Q is the measured volumetric flow rate and μ is the absolute viscosity of air. Using these two equations effective δp has been calculated and compared to the measured value at different pressure tap locations. This reveals that δp has a linear relationship with volumetric flow, indicating fully developed laminar flow.

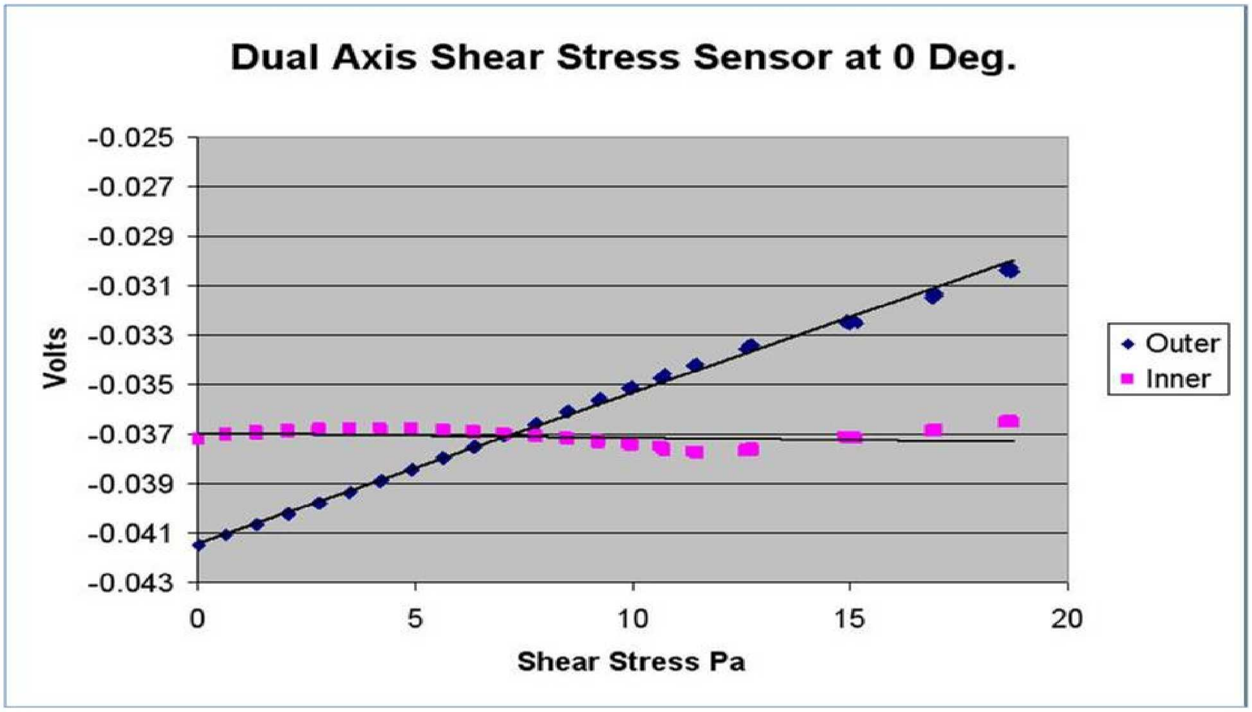

Figure 5 Two Component Sensor Data

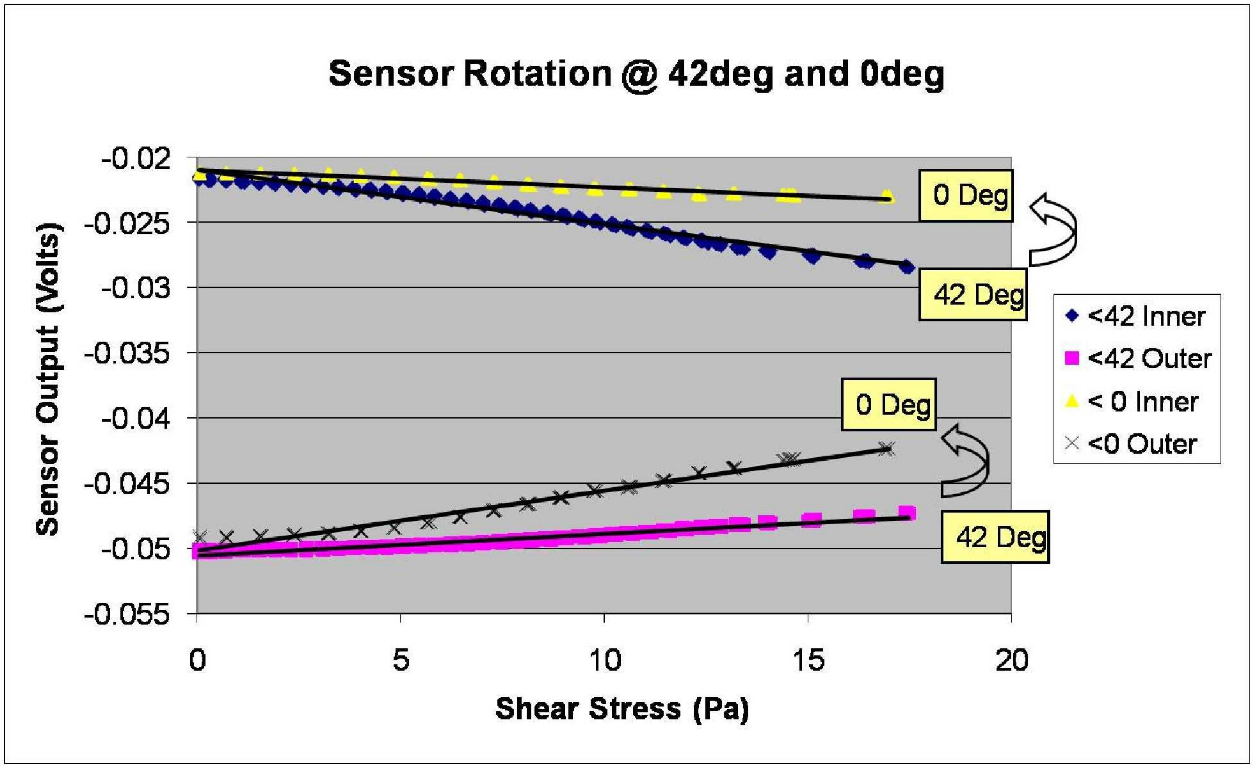

Figure 6 Two Comonent Rotational Results

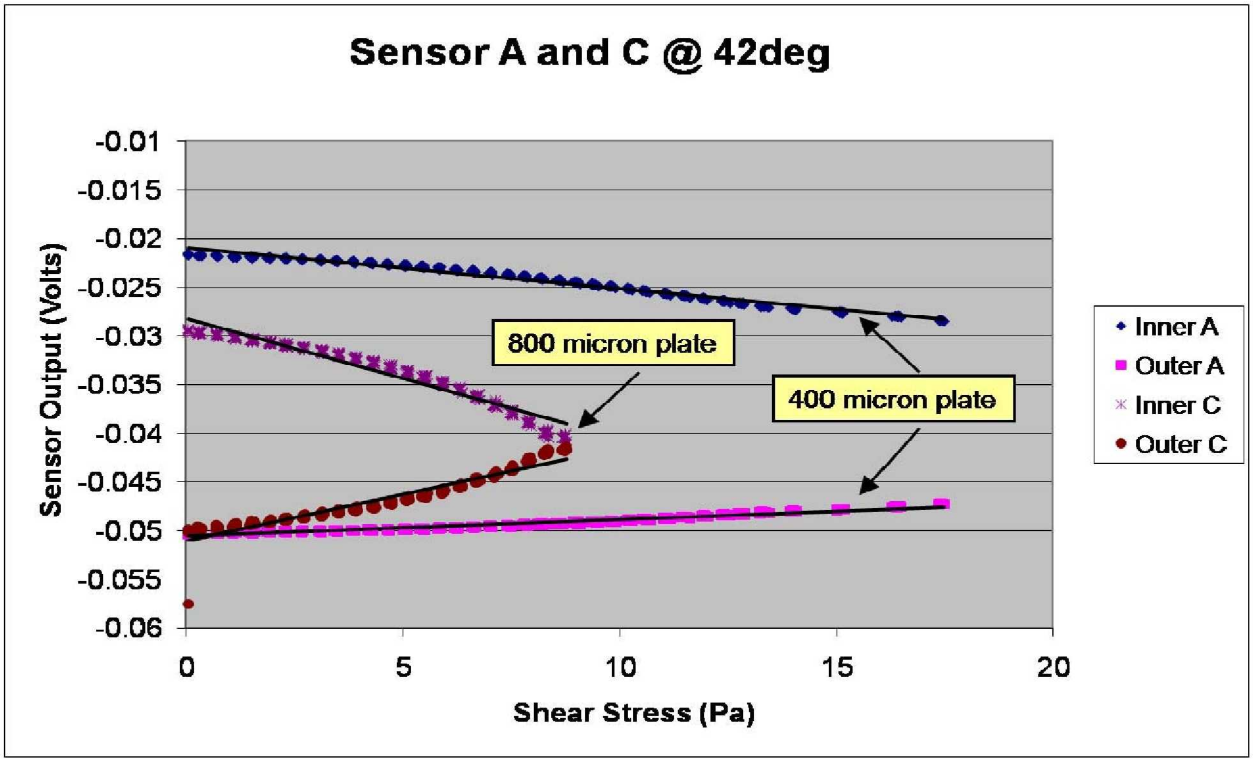

Figure 7 Varying Sensitivity with Plate Size

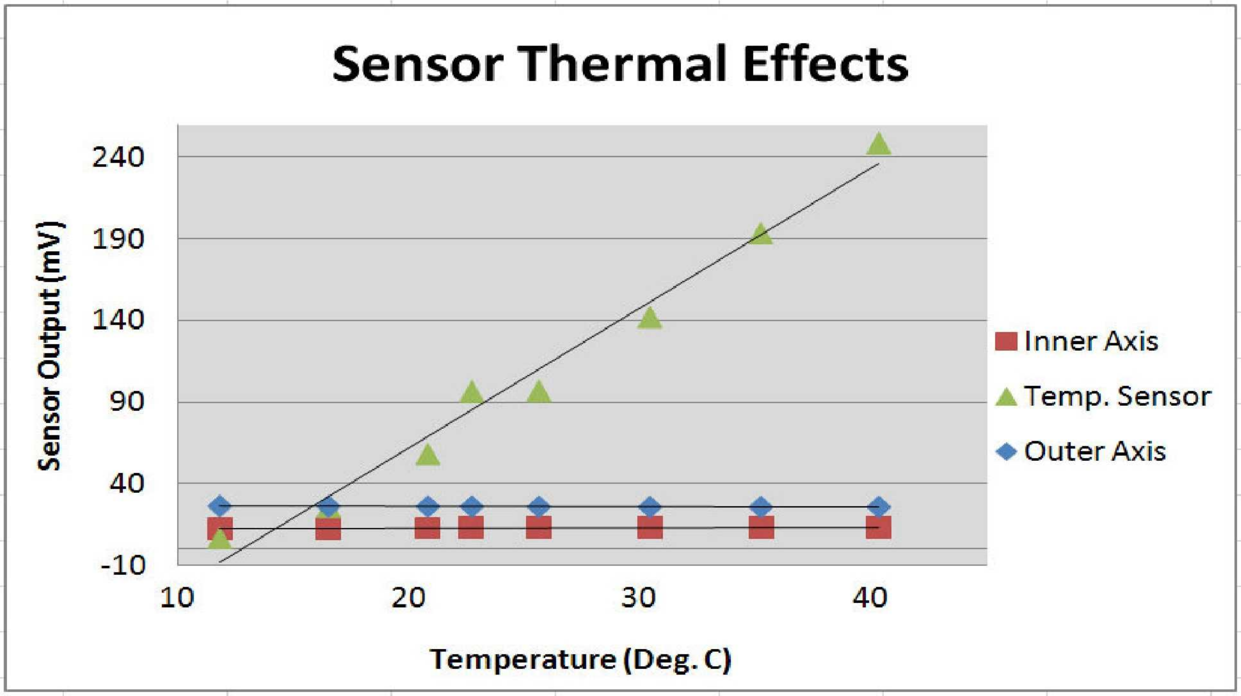

Figure 8 Thermal Effects on Sensors

Experimantal Results

Data was taken after a stable flow had been obtained; shear stress and sensor output voltage were displayed in real time. The sensor was powered by a constant current source (one for each axis) and the corresponding output voltage was recorded. (Figure 5) depicts data collected from one of these shear stress sensors. This sensor was oriented so that the outer axis was along the flow axis and the inner axis would be normal to the flow. As expected the sensor displayed a much higher sensitivity along the flow vector. The incident vector was varied by rotating the sensor mounting plug and both axis voltages were observed. (Figure 6) depicts the results of this rotation and as expected during each axis rotation the sensitivity increased as the sensor axis approached the flow direction. Several sensors were fabricated with varying plate diameters; this would in turn provide various shear ranges on the same silicon die. Figure 7 depicts data from such a die; this data shows the result of an 800µm and 400µm plate size. As expected the larger plate size provided data with increased sensitivity. These sensors were also thermally characterized, determining sensor signal thermal drift while also characterizing the on-die temperature sensor. (Figure 8) depicts the output of the on die temperature sensor as well as the output of the strain gauge. This graph shows that the "Greek Cross" [9] configuration of strain gauges has a much lower thermal sensitivity than a single strain gauge. The temperature sensor (composed of a single strain gauge) displays a linear response to temperature and proves suitable for on die temperature measurement.

The data shown here represents repeated runs of varying flow rates, consisting of hundreds of data points. Slight nonlinearities can be explained as variations in temperature during several hours of data collecting. Also errors due to azimuth misalignment in the flow channel could lead to some cross axis error. Other system induced errors could include reaching the lower limit of supporting instrumentation at low flow conditions, such as differential pressure along the flow cell and low value set points using the flow controller.

Summary

In summary, a need in the aerodynamic community to measure the forces on the surface due to skin friction or shear stress has been identified. A MEMS sensor has been introduced that directly measures shear stress in two axes. The device includes a force collecting plate that is in contact with the flow, a cantilever mount normal to the plate, a gimbal structure for two axes of movement, and imbedded strain gauges to convert mechanical shear into an electrical signal. The sensor is flush mounted with the flow surface, to keep from disrupting the natural aerodynamic effects. Also, the gimbal structure, arm, and plate are designed such that the tilt of the plate due to the shear stress does not impact the macroscopic flow parameters. To compliment this, all electrical leads and contacts are on the back side of the sensor and using a MEMS process to fabricate these devices lends to its high spatial resolution. This design has been fabricated and characterized with very favorable results as shown. Future work with these sensors includes further characterization, novel packaging for custom applications as well as other non-aerodynamic applications.

References

[1] Padmanabhan, A., Sheplak, M., Breuer, K.S., & Schmidt, M.A. "Micromachined sensors for static and dynamic shear-stress measurements in aerodynamic flows." *Proceedings of the IEEE Transducers '97 Conference*, Chicago, IL, June 1997. Lui, C,

[2] Pan, T., Hyman, D. Mehregany, M. Reshotko. E. & Willis, B. "Characterization of Microfabricated Shear Stress Sensors " 16th *International Congress on Instrumentation in Aerospace Simulation Facilities.* Dayton, OH, 1995.

[3] Sang, A. K,, Rolling, A. J., Schetz, J. A. "A Novel Skin Friction Sensor for Hypersonic Flow" *25th AIAA Aerodynamic Measurement Technology and Ground Testing Conference,* 5 - 8 June 2006, San Francisco, California

[4] Hakkinen, R. J., “Reflections on Fifty Years of Skin Friction Measurement” *24th AIAA Aerodynamic Measurement Technology and Ground Testing Conference* 28 June - 1 July 2004, Portland, Oregon

[5] Shi, S., Yi, L., Chen, D., Ou, Y., Jing, Y., Ye, T., Cheng, Z., “Two microthermal shear stress sensors: surface micromachined and bulk-bonding micromachined” *J. Micro/Nanolith. MEMS MOEMS 7(4), 043014* Oct–Dec 2008

[6] Naughton, J. W., and Sheplak, M., “Modern developments in shear-stress measurement” *Progress in Aerospace Sciences 38*, 2002, 521-527

[7] Scott, M. A., “The Need for a Shear Stress Calibration Standard” *24th AIAA Aerodynamic Measurement Technology and Ground Testing Conference* 28 June - 1 July 2004, Portland, Oregon

[8] F. Laermer and A. Schilp of Robert Bosch GmbH, "Method of Anisotropically Etching Silicon", US-Patent No. 5501 893

[9] Gridchin V.A., Gridchin A.V., Lubimsky V.M., Besedin V.M., “EXPERRWENTAL INVESTIGATION OF THE GREEK CROSS-SHAPED PIEZORESISTIVE ELEMENT” *4TH INTERNATIONAL CONFERENCE APEIE-98*

[10] Seebass, A. R., Bushnell, D. M., Hefner, J. N., “Viscous Drag Reduction in Boundary Layers” *Progress in Astronautics and Aeronautics,* Volume 123, August 1989

[11] Tiliakos, N., Papdopoulos, G., Modi, V., O’Grady, A., McCarhy, M., Frechette, L., Desbiens, J., Larger, R., “MEMS Shear Stress Sensor for Hypersonic Aeropropulsion Test and Evaluation” *2006 Annual ITEA Technology Review* August 710, 2006

[12] Schetz, J.A., "Skin Friction in Complex Turbulent Flows Using Direct Methods" Engineering Turbulence Modeling and Experiments 6 2005

REPORT DOCUMENTATION PAGE

Form Approved
OMB No. 0704-0188

1. REPORT DATE *(DD-MM-YYYY)*
01- 05 - 2010

2. REPORT TYPE
Technical Memorandum

3. DATES COVERED *(From - To)*

4. TITLE AND SUBTITLE
A Two-Axis Direct Fluid Shear Stress Sensor

5a. CONTRACT NUMBER

5b. GRANT NUMBER

5c. PROGRAM ELEMENT NUMBER

6. AUTHOR(S)
Adcock, Edward E.; Scott, Michael A.; Bajikar, Sateesh S.

5d. PROJECT NUMBER

5e. TASK NUMBER

5f. WORK UNIT NUMBER
698259.02.07.07.02.01

7. PERFORMING ORGANIZATION NAME(S) AND ADDRESS(ES)
NASA Langley Research Center
Hampton, VA 23681-2199

8. PERFORMING ORGANIZATION REPORT NUMBER
L-19878

9. SPONSORING/MONITORING AGENCY NAME(S) AND ADDRESS(ES)
National Aeronautics and Space Administration
Washington, DC 20546-0001

10. SPONSOR/MONITOR'S ACRONYM(S)
NASA

11. SPONSOR/MONITOR'S REPORT NUMBER(S)
NASA/TM-2010-216696

12. DISTRIBUTION/AVAILABILITY STATEMENT
Unclassified - Unlimited
Subject Category 35
Availability: NASA CASI (443) 757-5802

13. SUPPLEMENTARY NOTES

14. ABSTRACT

This innovation is a miniature or micro sized semiconductor sensor design that provides two axis direct non-intrusive measurement of skin friction or wall shear stress in fluid flow. The sensor is fabricated by micro-electro-mechanical system (MEMS) technology, enabling small size and low cost reproductions. The sensors have been fabricated by utilizing MEMS fabrication processes to bond a sensing element wafer to a fluid coupling wafer. This layering technique provides for an out of plane dimension that is on the same order of length as the in-plane dimensions. The sensor design has the following characteristics: a shear force collecting plate with dimensions that can be tailored to various application specific requirements such as spatial resolution, temporal resolution and shear force range and resolution. This plate is located coplanar to both the sensor body and flow boundary, and is connected to a dual axis gimbal structure by a connecting column or lever arm. The dual axis gimbal structure has torsional hinges with embedded piezoresistive torsional strain gauges which provide a voltage output that is correlated to the applied shear stress (and excitation current) on force collection plate that is located on the flow boundary surface (hence the transduction method). This combination of design elements create a “force concentration and resolution” structure that enables the generation of a large stress on the strain gauge from the small shear stress on the flow boundary wall. This design as well as the use of back side electrical contacts establishes a non-intrusive method to quantitatively measure the shear force vector on aerodynamic bodies.

15. SUBJECT TERMS
Boundary Layer; Laminar Flow Cell; MEMS; Shear Stress; Shear Vector; Skin Friction

16. SECURITY CLASSIFICATION OF:			**17. LIMITATION OF ABSTRACT**	**18. NUMBER OF PAGES**	**19a. NAME OF RESPONSIBLE PERSON**
a. REPORT	**b. ABSTRACT**	**c. THIS PAGE**			STI Help Desk (email: help@sti.nasa.gov)
					19b. TELEPHONE NUMBER ***(Include area code)***
U	U	U	UU	20	(443) 757-5802

Standard Form 298 (Rev. 8-98)
Prescribed by ANSI Std. Z39.18